

Mapping burned area in Alaska using MODIS data: a data limitations-driven modification to the regional burned area algorithm

Tatiana V. Loboda^{A,B}, Elizabeth E. Hoy^A, Louis Giglio^A and Eric S. Kasischke^A

^AGeography Department, University of Maryland, 2181 LeFrak Hall, College Park, MD 20742, USA.

^BCorresponding author. Email: loboda@umd.edu

Abstract. With the recently observed and projected trends of growing wildland fire occurrence in high northern latitudes, satellite-based burned area mapping in these regions is becoming increasingly important for scientific and fire management communities. Coarse- and moderate-resolution remotely sensed data products are the only viable source of comprehensive and timely estimates of burned area in remote, sparsely populated regions. Several MODIS (Moderate Resolution Imaging Spectroradiometer)-based burned area products for Alaska are currently available. However, our research shows that the existing burned area products underestimate the extent of the effect of fire by 15–70%. Environmental conditions limit the effective observation of land surface in Alaska to the period between May and September. These limitations are particularly noticeable in mapping late-season fires. Here we present an ecosystem-based modification to a previously developed burned area mapping approach designed to enhance the algorithm performance in Alaska. The mapping results show a consistently high performance of the adjusted algorithm in mapping burned areas in Alaska during large (2004 and 2005) and small (2006 and 2007) fire years. The adjusted burned area product maps burned areas identified by the Monitoring Trends in Burn Severity products with the overall accuracy of 90–93% and Kappa of 0.67–0.75%.

Additional keywords: boreal forest, high northern latitudes, wildland fire.

Introduction

High northern latitudes of North America, and Alaska in particular, have seen a dramatic increase in fire occurrence over the past several decades. Scientists are reporting an increase in the total area burned (Gillett *et al.* 2004) and frequency of large fire seasons (Kasischke and Turetsky 2006; Soja *et al.* 2007; Ivanova *et al.* 2010) across the boreal region. Wildland fires occur in remote and inaccessible areas, making them particularly difficult to monitor and map using field techniques and increasingly more expensive in terms of aerial-based assessment. At the same time, satellite-based remote sensing offers practical solutions for development of a long-term, consistent, detailed and unbiased record of fire activity in this region.

Several satellite-based fire monitoring programs and products are currently available to the fire management and scientific community. These include daily observations of on-going fire activity from the Moderate Resolution Imaging Spectroradiometer (MODIS) active fire product (Giglio *et al.* 2003), monthly records of burned area from the provisional global MODIS burned area product (Roy *et al.* 2005, 2008), Landsat-based burn severity estimates produced within the Monitoring Trends in Burn Severity (MTBS) program (see <http://mtbs.gov/>, accessed 27 August 2010), and data products from analysis of AVHRR (Advanced Very High Resolution Radiometer) data (Pu *et al.* 2007; Chuvieco *et al.* 2008).

Although the suite of available products includes coarse- (1 km), moderate- (250–500 m), and high- (30 m) resolution observations, only coarse- and moderate-resolution data provide a feasible method for obtaining timely information about the spatial extent of fire occurrence during the fire season or immediately following the fire season as data availability of cloud-free observations at high resolution is limited (Verbyla *et al.* 2008).

The MODIS instrument on board the polar orbiting Terra and Aqua satellites offers enhanced opportunities for fire observations (Kaufman *et al.* 1998). The suite of standard MODIS products includes global active fire observations (Giglio *et al.* 2003) and the provisional global MODIS burned area product (Roy *et al.* 2005, 2008), as well as surface reflectance datasets from which custom ecosystem-specific burned area products have been developed (e.g. Loboda *et al.* 2007). The expected continuity of moderate- to coarse-resolution satellite data that will be available through the launch of the Visible Infrared Imaging Radiometer Suite (VIIRS) on the National Polar-orbiting Operational Environmental Satellite System (NPOESS) positions these products and methodologies to become a reliable long-term source of fire-related information in the future.

Despite the advantages offered by high-frequency coverage of high northern latitudes from coarse- and moderate-resolution

polar orbiting satellites, there are several environmental constraints on satellite-derived observations of surface area in these regions. One of the most pronounced limitations for using reflected visible and infrared radiation at high northern latitudes is defined by the seasonal variation of incoming solar radiation due to high solar zenith angles (SZAs). Regions above 60°N receive little or no incoming solar radiation during several months within a year. During the months when polar areas receive a substantial amount of solar radiation, the SZA is high. High SZAs minimise the amount of incoming solar radiation reaching the surface in two important ways. First, the amount of incoming radiation per unit area decreases as a function of cosine of SZA (Schott 1997). Consequently, with the rising SZA from 0° to 30°, 60°, 75° and 80°, the total amount of incoming solar radiation fraction per unit area drops sharply from 1 to 0.87, 0.5, 0.26 and 0.17 respectively. Second, the amount of solar radiance reaching the surface is further decreased with the lengthening of the path of incoming solar radiation through the atmosphere, where it interacts with gases and aerosols and is absorbed, reflected and scattered (Schott 1997). Finally, high SZAs contribute to the increased amount of topographic shadowing and thus further limit the amount of clearly observable land surface (Verbyla *et al.* 2008).

In addition to limitations imposed by variability in solar illumination, burned area mapping efforts are impeded by smoke-related high aerosol concentrations, cloud cover, cloud shadow and snow cover when direct observations of land-surface characteristics are unavailable. Smoke poses a challenging problem as fires in Alaska and other high northern latitudes tend to burn for an extended period of time, effectively masking areas burned for a significant portion of the snow-free season. This problem is particularly challenging during late-season fires when burned areas are quickly covered with snow and remain masked until the following year. Furthermore, the compound effects of snowmelt, snowmelt-induced flooding and early vegetation senescence alter surface reflectance signatures, which frequently resemble those of burned areas (Roy *et al.* 2005).

The goal of this study was to carry out an assessment of various burned area mapping approaches that can be applied to MODIS data, evaluate regional characteristics of fire occurrence from the MODIS active fire observations, and define limitations in data availability of land-surface observations in order to develop an understanding of burned area mapping challenges in Alaska and develop an adjustment to the existing regional MODIS-based algorithm (Loboda *et al.* 2007) to improve the accuracy of burned area mapping in Alaska. The initial step in our study ('Environmental challenges in satellite mapping of burned area in Alaska and other high northern latitudes' section) was an evaluation of fire regimes in Alaska and an assessment of factors limiting the use of MODIS data for mapping burned area in high northern latitude regions. The 'Burned area estimates for Alaska from existing MODIS products and algorithms' section presents a comparison of three MODIS-based burned area products for the 2004 fire season in Alaska. Based on the presented assessments, we modified the approach of Loboda *et al.* (2007) to include processing of MODIS data from the spring of the year following the fires. This portion of the study is presented in the 'Algorithm

modifications for the regional burned area product specific to Alaska' section.

Environmental challenges in satellite mapping of burned area in Alaska and other high northern latitudes

This study focussed on mapping burned areas in Alaska that were contained within MODIS tiles h10v02, h11v02 and h12v02 (Wolfe *et al.* 1998), which fully cover the interior region of the state where most wildland fires occur (Kasischke *et al.* 2002) (Fig. 1). To identify the specific challenges of burned area mapping from remotely sensed data in high northern latitudes, we evaluated primary and auxiliary information available in two standard MODIS products for data collected from 2003 to 2007. We used the Collection 5 MODIS active fire product (MOD14A1 and MYD14A1) (Giglio *et al.* 2003) to provide an assessment of observed fire activity during this period (described in the 'Fire season characteristics' section). In addition, we used auxiliary information provided within the Collection 5 MODIS 8-day surface reflectance composites (MOD09A1) (Vermote *et al.* 2002) to describe environmental conditions enabling or impeding observations of land surface in the study area ('Constraints on using MODIS land-surface observations for burned area mapping in high northern latitudes' section).

Fire season characteristics

Our analysis of active fire detections derived from the MODIS data across all of Alaska demonstrated that the majority of fire activity (on average ~90% of all fire detections annually between 2004 and 2007) is concentrated in interior Alaska between 60° and 70°N, supporting previously reported estimates (Kasischke *et al.* 2002). The present analysis also showed that the primary fire season in Alaska occurred during 3 months of the year – June, July and August. Between 2003 and 2007, 99% of all fire detections were recorded during June–August, with August detections accounting for ~48% of the 5-year total. The high percentages of late-season fires were driven by the extremely large events during 2004 and 2005 seasons that together accounted for 91% of all fire detections between 2003 and 2007. Despite the differences in the total amount of fire activity, the intra-annual dynamics of fire occurrence followed the same pattern for all years. Although overall few fires were detected before June, in 2007 nearly 7% of all detected fires occurred in May, and in some years (2005, 2006) small fires were observed as early as April. The majority of fires were out by the end of August, with few fires continuing into September. The 2007 fire season presents an exception because one of the largest fires during that year burned through the end of September. However, during the 5-year period, September fires accounted for ~2% and spring fires accounted for less than 0.5% of all MODIS fire detections.

Constraints on using MODIS land-surface observations for burned area mapping in Alaska and other high northern latitudes

The MODIS 8-day surface reflectance composites product retains auxiliary information about the SZA of a pixel at the time of image acquisition. We used these data to analyse the mean SZA of remotely sensed data during the 2003–07 period by

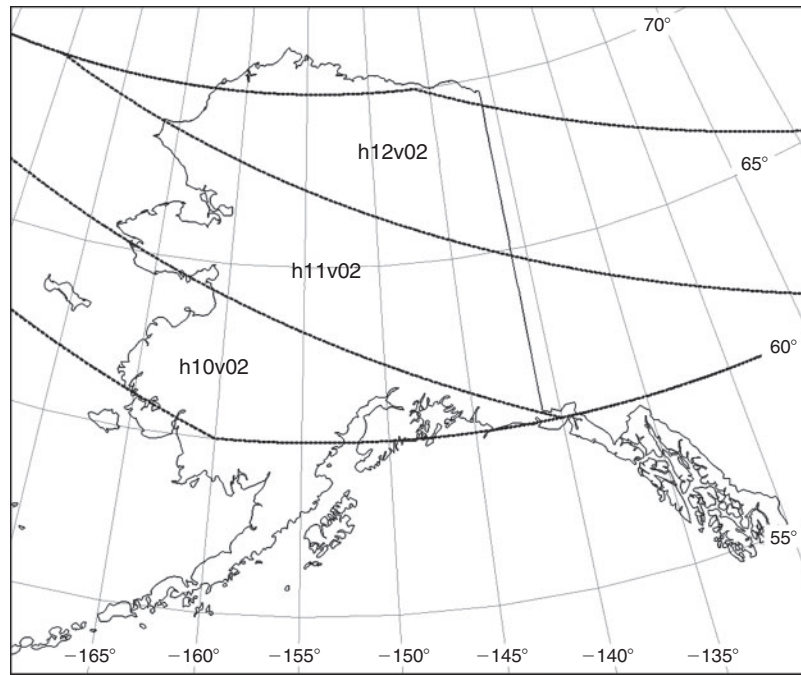


Fig. 1. Geographic extent of the study area within the MODIS (Moderate Resolution Imaging Spectroradiometer) tiles h10v02, h11v02 and h12v02. The MODIS tiles are reprojected from their native sinusoidal projection to the Albers conical equal area projection for Alaska.

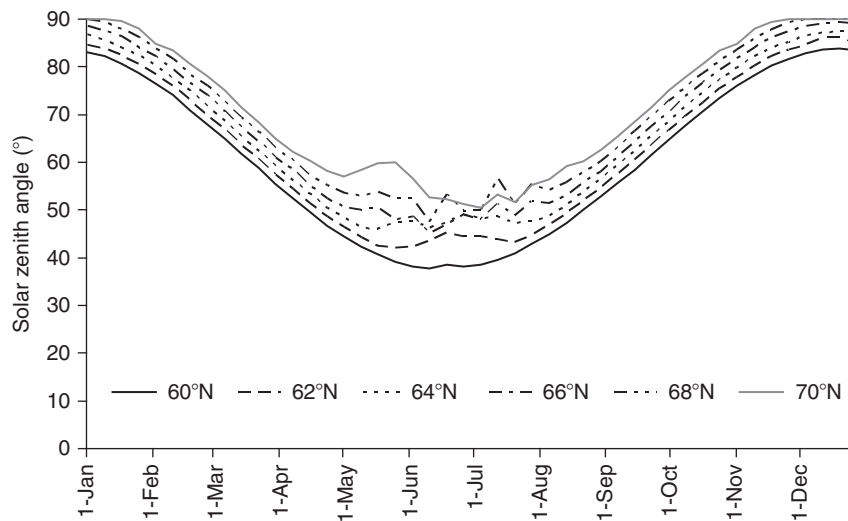


Fig. 2. Five-year mean seasonal change in solar zenith angles (SZAs) of remotely sensed observations acquired by the MODIS (Moderate Resolution Imaging Spectroradiometer) instrument as summarised in the Collection 5 MOD09A1 product in Alaska. The lines represent 5-year mean SZAs at various parallels between 60° and 70°N.

latitude (Fig. 2). Because of the overlap of satellite orbits in the high northern latitudes, the MODIS sensor on board the same satellite (Terra) can acquire images of the same area at different local overpass times, thus resulting in variability of the SZA not only due to the seasonal change but due to the time of acquisition as well. The SZA has a direct and considerable effect on observations of vegetation. Several studies noted the SZA-driven signal modification in visible and near-infrared

wavelengths particularly above 70° SZA, and it has been suggested that observations at 80° SZA and greater should be discarded (Holben 1986; Deng and Di 2001; Chen *et al.* 2003). The most optimal vegetation observation conditions at $SZA \leq 60^\circ$ (Singh 1988) occur between the beginning of April and the beginning of September with an ~30-day shorter period at the northern (70°N) boundary and ~30-day longer period at the southern (60°N) boundary.

In addition to SZA-induced limitations, the quality of MODIS-based surface observations is strongly influenced by atmospheric and other environmental conditions such as cloud cover and cloud shadow, the amount of aerosols in the atmospheric column, and the presence of snow on the ground. We used the MOD09A1 500-m quality state flags information to evaluate the 5-year mean (2003–07) intra-annual trajectories of these conditions in Alaska. Table 1 lists respective unpacked bits and accepted values used in evaluation of those parameters. We limited the analysis to the evaluation of conditions over the land surface only and expressed them as percentage of total land surface within each category. Fig. 3 shows that the entire state of Alaska is snow-free only between early June and the beginning of September. Snow-melt and snow-establishment are rapid events, lasting on average 1 month during May and September respectively.

During the snow-free period, high aerosol concentrations, partially due to on-going wildland fires, obscure 30–35% of the

land area (Fig. 3). Cloud and cloud-shadow interference during the summer months is relatively low (<20% of land area). The amount of clearly observable surface drops to ~37 and ~50% in May and September respectively, and then goes below 20% from October through April (Fig. 4). The reduction in the availability of uncontaminated MODIS imagery later in the fire season reduces the effectiveness of algorithms that use data only from the same year that the fire occurred, especially during large-fire years when late-season burning is common.

Burned area estimates for Alaska from existing MODIS products and algorithms

For fire events that occurred in 2004, we compared end-of-season burned area maps from the MODIS Collection 5 provisional burned area product (MCD45A1) (Roy *et al.* 2008), the MODIS direct broadcast burned area product (Giglio *et al.* 2009), and a regional MODIS burned area product generated through using the approach of Loboda *et al.* (2007) with the MTBS dataset that was generated through analysis of Landsat Thematic Mapper (TM) and Enhanced Thematic Mapper Plus (ETM+) data. The MODIS Collection 5 provisional burned area product uses MODIS surface reflectance data to provide the approximate day of burning or unburned information for each 500-m pixel (Roy *et al.* 2008). The MODIS direct broadcast burned area product combines MODIS surface reflectance data with the MODIS active fire product and the MODIS land-cover product to provide the approximate day of burning or unburned information for each 500-m pixel (Giglio *et al.* 2009). The regional MODIS burned area product combines MODIS surface reflectance data with the MODIS active fire product to provide a region-specific approximate day of burning or unburned information for each 500-m pixel (Loboda *et al.* 2007). In Alaska, the MTBS dataset includes spatially explicit burn scars greater than 404 ha (1000 acres) classified into several burn severity categories (Eidenshink *et al.* 2007). In the present assessment, we used the MTBS differenced Normalised Burn Ratio (dNBR)

Table 1. Accepted values from the MOD09A1 500-m Surface Reflectance Data State (500-m state flags) packed bit layer for the analysis of the environmental conditions and identification of clear land surface for burned area mapping

Bit number	Parameter name	Accepted values	
		Environmental conditions analysis	Clear land surface
0–1	MOD35 cloud	1–2	0, 3
2	Cloud shadow	1	0
3–4	Land or water flag	1	1
6–7	Aerosol quantity	0, 3	1, 2
8–9	Cirrus detected	3	0–2
10	Internal cloud flag	1	0
11	Internal fire flag		0
12	MOD35 snow or ice	1	0
15	Internal snow or ice	1	0

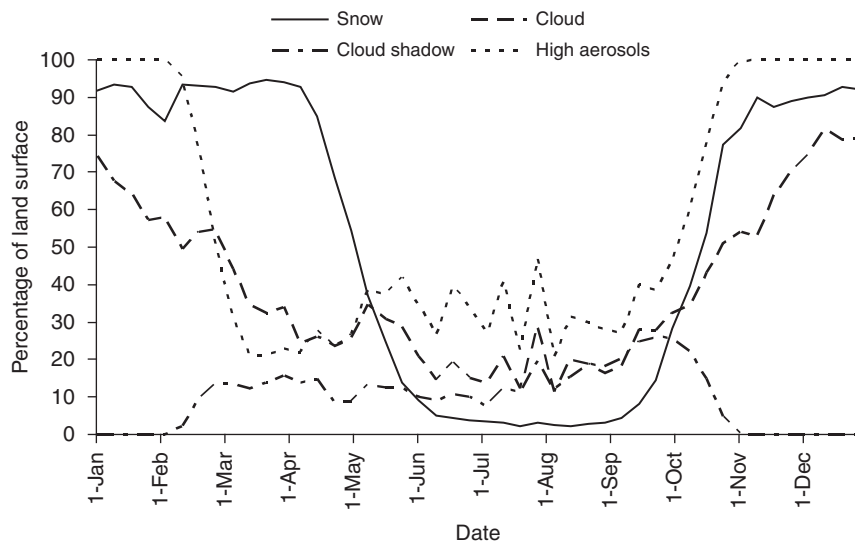


Fig. 3. Five-year mean seasonal trajectories of the presence of cloud cover, cloud shadow, aerosols and snow cover from the Collection 5 MOD09A1 500-m quality state flags.

(López García and Caselles 1991) product, which allowed us to separate ‘burned’ from ‘unburned’ categories within the MTBS perimeters according to the scheme presented in Table 2. We further used confusion matrices to evaluate mapping accuracy for various MODIS-based algorithms within the MTBS analysis area (Fig. 5). More information about each burned area product and associated algorithm can be found in the respective articles cited.

The analysis showed that all existing MODIS-based algorithms included in this comparison underestimated burned area in Alaska in 2004 (Table 3). All three MODIS products under-reported burned area when compared with the Landsat-based estimates. The major source of the underestimation of burned area resulted from one very large scar (298 188 ha) representing a late-season fire still burning in September (mapped by the MODIS active fire product) (Fig. 6). In this case, burning continued through the middle of September, thus leaving a limited time-window after fire occurrence to collect the MODIS data required to map the areal extent of the burn within the same season as required by all MODIS-based algorithms assessed in this study.

In addition to the per-pixel assessment of mapping accuracy provided above, we assessed reported burned area estimates per individual fire scar compared with the MTBS perimeters (Table 4, Fig. 7). Although the MTBS perimeters include unburned islands, this analysis allows for a better comparison of fire-affected area than the MTBS dNBR products, which incorporate mapping gaps due to cloud presence and Landsat 7 Scan Line Corrector (SLC Off) artefacts (Fig. 5). According to the results of this intercomparison, all three MODIS products under-reported burned area when compared with the Landsat-based estimates: by 70% for the MODIS provisional burned area product, by 24% for the MODIS direct broadcast algorithm, and by 15% for the regional MODIS algorithm. It was expected that regionally adapted burned area thresholds would yield more accurate results compared with the global products of the MODIS Collection 5 provisional burned area product and the

MODIS direct broadcast burned area product. The analysis also showed that the major source of underestimation was in mapping extremely large burn events, and that the reported accuracy improves as the size of individual burns decreases. For all fire events under 100 000 ha, the MODIS-based estimates improve for all products to 60, 12 and 9% underestimation for the provisional burned area, direct broadcast, and regional algorithms respectively. This finding sounds counterintuitive and appears to contradict results of previous studies that show that mapping accuracy from moderate-resolution data sources increases with an increase in burn scar size (Fraser *et al.* 2000; Pu *et al.* 2007). However, subsequent evaluation revealed that the accuracy of burned area estimates was not driven as much by the size of the burn as by the late-season timing of burning during the year effectively closing the mapping window for the ‘end-of-the year’ mapping approaches.

Algorithm modifications for the regional burned area product specific to Alaska

Methods

The analysis of environmental conditions in high northern latitudes indicates that late-season fires are unlikely to be mapped

Table 2. Reclassification scheme for the Monitoring Trends in Burn Severity (MTBS) burn severity classes for the burned area accuracy assessment

Input class	Definition	Output class
0	Unburned, outside perimeter	Unburned
1	Unburned to low severity	Unburned
2	Low severity	Burned
3	Moderate severity	Burned
4	High severity	Burned
5	Increased greenness	Excluded
6	Non-processing area mask	Excluded

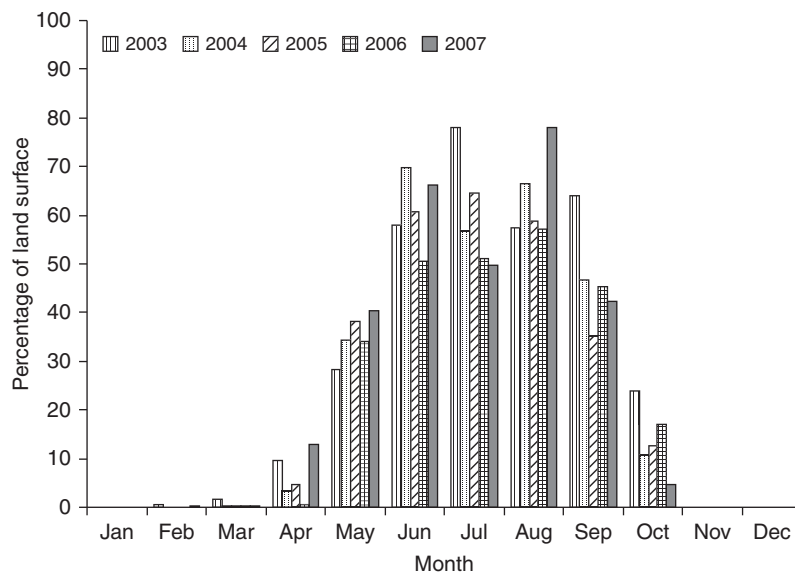


Fig. 4. Interannual variability in clear land-surface observations from the Collection 5 MOD09A1 500-m quality state flags between 2003 and 2007.

by any algorithm based on a fixed time-window of post-fire surface observations limited to the same year. One possible solution, which was previously suggested for mapping burned area in Alaska using AVHRR data (Kasischke and French 1995), includes adding the following year's spring composite to fill in

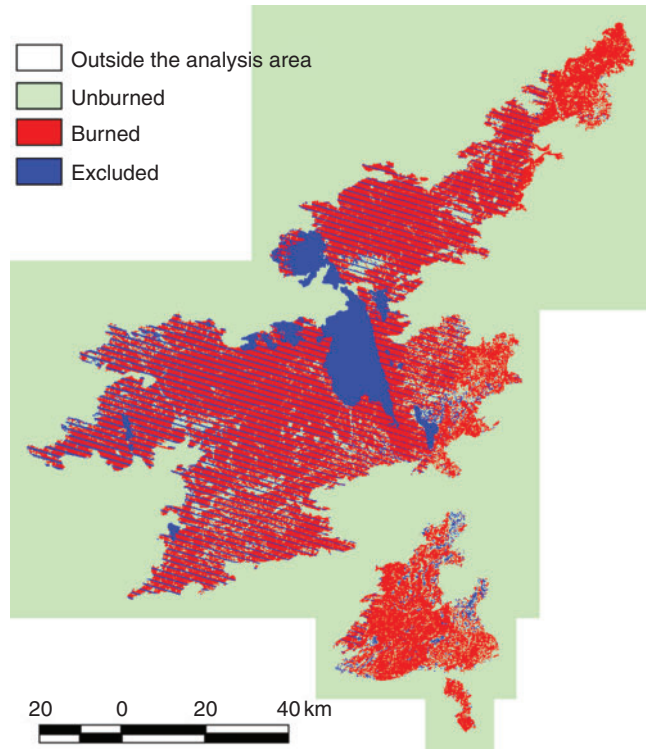


Fig. 5. Reclassified Monitoring Trends in Burn Severity (MTBS) data products and their components used in the assessment of MODIS (Moderate Resolution Imaging Spectroradiometer)-based algorithm performance.

the gaps left by the lack of sufficient clear surface observations during the given fire season. In order to optimise mapping accuracy of the regional MODIS burned area algorithm for Alaska, we modified the original Loboda *et al.* (2007) methodology to include pre-season and post-season spring composites as described below.

First, burned areas were mapped following the original methodology of Loboda *et al.* (2007). This methodology is based on semi-automated processing of standard MODIS land products into burned area maps using information about changes in surface reflectance due to fire and the record of fire activity. The algorithm ingests the MODIS 500-m 8-day surface reflectance composites (MOD09A1) (Vermote *et al.* 2002) collected during the year of interest and the year before, masks out poor-quality data using MOD09A1 quality bits, and produces 8-day dNBR grids. A set of vegetation-dependent dNBR thresholds is then developed by an analyst to reflect ecosystem-specific changes in surface reflectance due to fire. These masks of potential burning, created by separating the dNBR grids into ‘potentially burned’ and ‘unburned’ categories, are further compared with the observed fire activity recorded by the MODIS active fire detections (Giglio *et al.* 2003) to eliminate instances of surface reflectance change due to reasons other than fire. At this stage, two thresholds are set for active fire detections included in the analysis: (1) the area threshold that defines a minimum of active fires detections per unit burned area, and (2) the temporal threshold, which is defined by the longevity of a burn scar, the possible length of a fire-event occurrence, and the possible length of a period of persistent cloud cover impeding surface observations. Finally, the resultant 8-day burn masks are merged into an end-of-season burned area product. With the changes introduced in the MODIS Collection 5 reprocessing, new updates to acceptability of pixels for burned area mapping were defined (Table 1). Spatial and temporal thresholds were determined using a sample of known burned area within Alaskan boreal

Table 3. Summary of confusion matrix results comparing moderate resolution MODIS (Moderate Resolution Imaging Spectroradiometer)-based products, including provisional burned area (Prov BA) algorithm, direct broadcast burned area (DB) and regional burned area (Reg BA) algorithm, with MTBS (Monitoring Trends in Burn Severity) burns for 2004 fire season and multiyear comparison of the regional adjusted algorithm with MTBS burns between 2004 and 2007

		Producer accuracy (%)	User accuracy (%)	Overall accuracy (%)	Kappa
Prov BA	Unburned	97.86	81.79	81.86	0.37
	Burned	31.69	82.56		
DB	Unburned	92.73	92.77	89.01	0.7
	Burned	77.35	77.26		
Reg BA	Unburned	91.12	93.27	88.28	0.69
	Burned	79.38	74.05		
Regional adjusted burned area mapping algorithm					
2004 (<i>n</i> = 78 943 176)	Unburned	89.57	97.06	90.03	0.75
	Burned	91.5	73.68		
2005 (<i>n</i> = 69 612 885)	Unburned	91.05	97.19	90.97	0.76
	Burned	90.69	74.11		
2006 (<i>n</i> = 5 380 676)	Unburned	92.95	97.39	91.69	0.67
	Burned	83.15	63.57		
2007 (<i>n</i> = 13 246 336)	Unburned	93.83	97.96	93	0.73
	Burned	87.8	69.5		

forests obtained from MTBS Landsat scenes following the methodology described in Loboda *et al.* (2007). Regional dNBR thresholds were established at 0.25 and 0.2 for areas with tree cover >10% and ≤10% respectively. MODIS pixels with values above those thresholds were considered potentially burned. The potentially burned pixels were further compared with the active fire detection to ensure that the observed change in surface reflectance occurred owing to burning. The active fire detection thresholds, designed to limit the selection of appropriate samples of active fires from the

MODIS active fire product, were set at three times the area mapped by active fires for the area threshold and 64 days before the date of the given composite for the temporal threshold. For a more complete description of threshold identification, see Loboda *et al.* (2007).

The spring composite was automatically created from the MODIS 8-day composite files acquired during late April–May (composite Julian Dates (JD) 121–153) to develop a pre-fire-season clear surface view. The analysis of active fire detections (see ‘Fire season characteristics’ section) showed that few fires

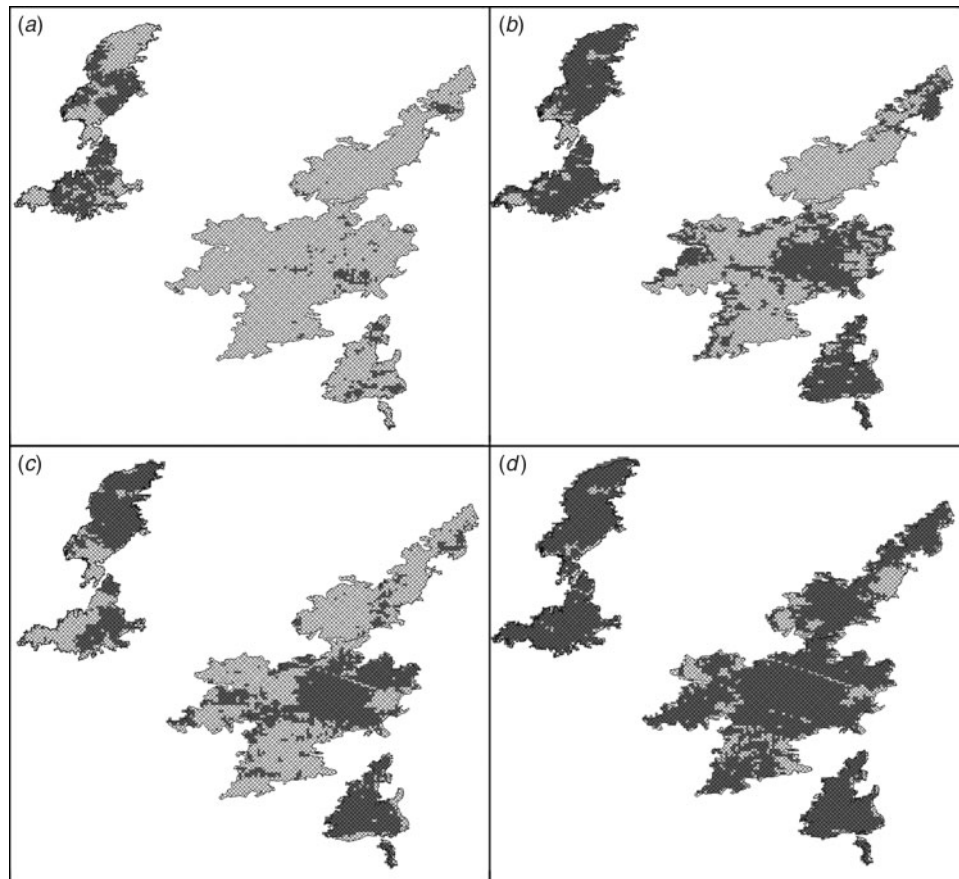


Fig. 6. Comparison of Monitoring Trends in Burn Severity (MTBS) scar with: (a) MODIS (Moderate Resolution Imaging Spectroradiometer) provisional burned area; (b) MODIS direct broadcast algorithm; (c) regional MODIS burned area algorithm; and (d) adjusted regional MODIS burned area algorithm. MTBS burn perimeters are cross-hatched black and MODIS-based burned area products are shown in solid grey.

Table 4. Summary of regression model results comparing moderate-resolution MODIS (Moderate Resolution Imaging Spectroradiometer)-based products, including provisional burned area (Prov BA) algorithm, direct broadcast burned area (DB) and regional adjusted (Reg BA) algorithm, with MTBS (Monitoring Trends in Burn Severity) fire perimeters for 2004 fire season

Product	Regression model			Regression coefficient			
	R^2	F statistic	Significance	Coefficient	t statistic	95% confidence interval	Significance
Prov BA	0.81	287.5	$P < 0.0001$	0.302	17.0	±0.036	$P < 0.0001$
DB	0.92	983.3	$P < 0.0001$	0.764	31.6	±0.048	$P < 0.0001$
Reg BA	0.93	942.3	$P < 0.0001$	0.851	30.7	±0.055	$P < 0.0001$

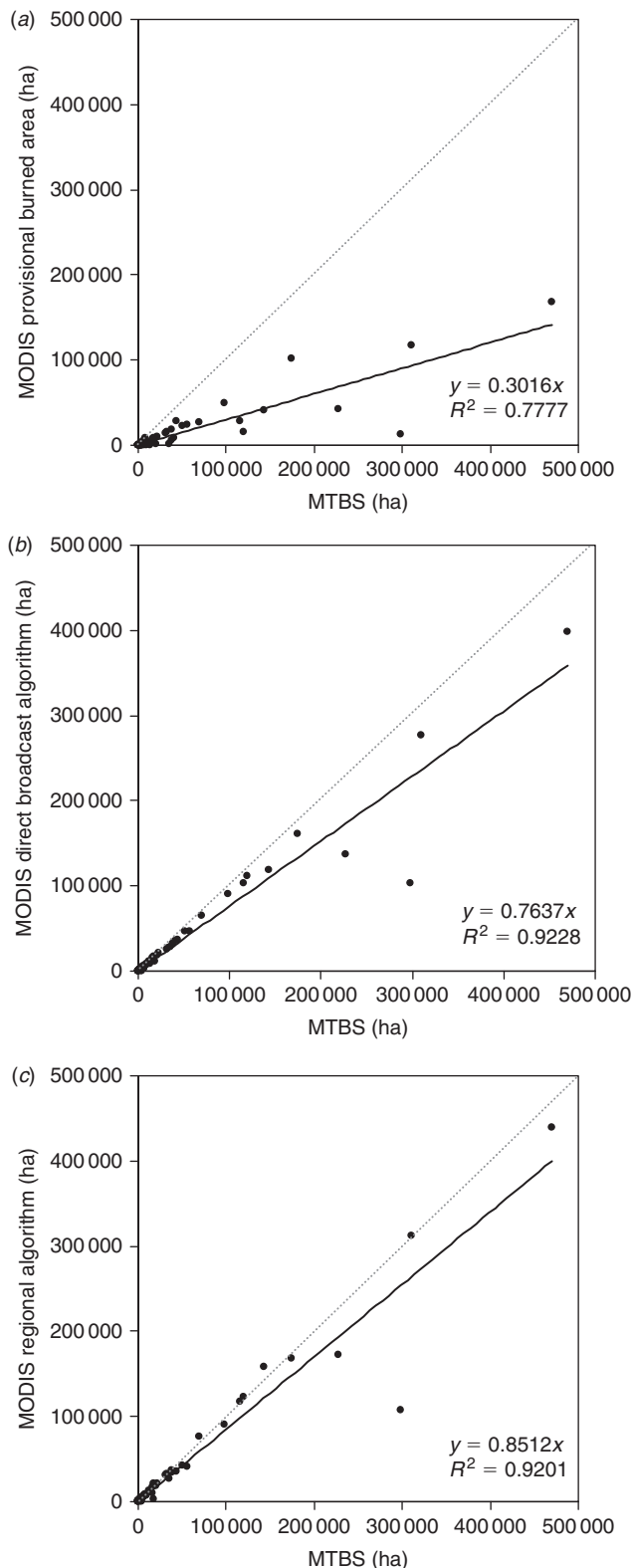


Fig. 7. Comparison of MODIS (Moderate Resolution Imaging Spectroradiometer)-based burned area products ((a) MODIS provisional burned area; (b) MODIS direct broadcast algorithm; and (c) regional MODIS burned area algorithm) with Monitoring Trends in Burn Severity (MTBS) burn perimeters for 2004 fire season ($P < 0.0001$).

occurred during this time and they were easily separated from the fire scars of the previous year. The JD 153 MODIS 8-day composite was then modified using the information contained in the quality layer to mask out pixels of low quality (Table 1). The masked-out pixels from the base composite were filled with acceptable-quality pixels from the composite of the previous date (JD 8). The process was repeated until the JD reached 121, after which the remaining poor-quality pixels were permanently masked out. The JD 121 cut-off date was based on the snow-melt trajectories described in the 'Constraints on using MODIS land-surface observations for burned area mapping in Alaska and other high northern latitudes' section.

Visual analysis of multiyear burned area mapping using the original regional burned area algorithm showed that new burn scars were frequently found to be adjacent to the burns from the previous year. To eliminate the potential confusion in the year of burning, a pre-fire-season spring composite was created to exclude previously burned areas. MODIS09A1 composites between JD 121 and 153 were combined in a single clear-surface pre-burn composite for year, and year_{*i*-1} with preferential selection of later dates in the compositing time-window. The subsequent processing included analysis of three spring composites: the spring pre-fire-season composite (year_{*i*}), the spring post-fire season composite of the following year (year_{*i*+1}), and the spring pre-fire-season composite of the previous year (year_{*i*-1}). dNBR images were calculated for composites from (1) year_{*i*-1} and year_{*i*}, and (2) year_{*i*} and year_{*i*+1}. The dNBR images were further processed using the regional thresholds developed for Alaska and using cumulative fire detections from the previous year for the pre-fire-season dNBR composite and from the current fire season for the post-fire dNBR composite. The resultant burned area masks from the post-fire season were merged with the burns mapped using the original algorithm. Finally, the pre-fire-season masks were erased from the resultant product. Fig. 8 shows the overall flow of the adjusted regional burned area mapping algorithm.

Accuracy assessment

We applied the adjusted regional algorithm to the MODIS data for four fire seasons (2004–07) to test the interannual stability of algorithm performance during large (2004 and 2005) and small (2006 and 2007) fire years. The MODIS-based burned area maps were compared with the MTBS fire scars produced for 2004–07. We applied dNBR-based thresholds provided within the MTBS products and reclassified the MTBS product following the scheme presented in Table 2 to identify burned and unburned areas, and areas excluded from the analysis. We further compared burned and unburned categories within each class at the MTBS resolution (30 m) through confusion matrices.

The results show that the adjusted regional algorithm improved burned area estimates for Alaska during the 2004 fire season from $Kappa = 0.69$ to $Kappa = 0.75$ (Table 3). Although the statistical estimates appear to reflect relatively small improvements in the algorithm's mapping accuracy, visual examination reveals a considerable success in improving the completeness of burned area mapping, particularly for late-season fires (Fig. 6*d*). The performance of the algorithm was stable from 2004 to 2007, with the overall accuracy of burned

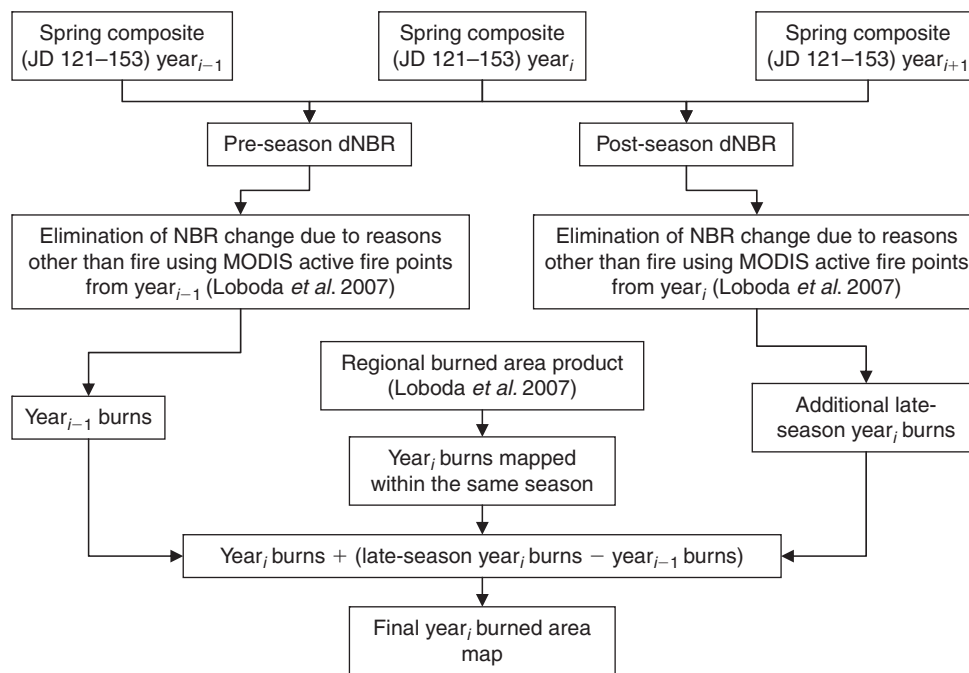


Fig. 8. Overall flow of the adjusted regional burned area mapping algorithm for Alaska (dNBR, differenced Normalised Burn Ratio).

area estimates ranging between 90 and 93% and Kappa values ranging between 0.67 and 0.76 during 2004–07. The Producer and User Accuracies are consistent in the product between the years. The ‘burned’ class commission error is the most significant source of disagreement between the MTBS estimates and those produced by the adjusted regional MODIS algorithm. In most instances, the commission error is attributed to the edge effect of the moderate-resolution MODIS pixels and to the internal variability of burn within a single MODIS pixel. Spatial aggregation effects are known to increase total burned area in moderate- and coarse-resolution products (Fraser *et al.* 2004), and the scale difference between MODIS-based products and the Landsat-based validation set explains some of the error (Eva and Lambin 1998). However, in some cases the ‘commission’ error in the burned area class is a result of missing burn maps in the MTBS dataset. Although the MTBS dataset only includes scars with area greater than 404 ha, the adjusted regional MODIS burned area algorithm includes all burns within the unburned areas of the MTBS dataset.

We attribute the variation in performance between the MODIS Collection 5 provisional burned area product, the MODIS direct broadcast burned area product, the regional MODIS burned area product and the adapted regional MODIS burned area product to differences in approach and input data. The provisional burned area product is the only one of the set that does not use the MODIS active fire product and is based solely on changes in surface reflectance. The MODIS direct broadcast product is based on changes within a 10-day window, and if no clear observations are available owing to smoke-related high aerosol concentrations or cloud cover, then the pixel may not be mapped as burned. Both of these products are global and therefore do not focus on regional specifics. A version of the

regional MODIS burned area product was developed for use in central Siberian boreal forests and focusses on specifics of boreal ecosystems while taking advantage of changes in surface reflectance and active fire detections within ecosystem context. However, the adjusted MODIS burned area product improves on that algorithm by solving the issues of missed burned pixels due to smoke-related high aerosol concentrations or cloud cover and late-season burning.

Conclusions

Moderate-resolution remotely sensed burned area products are important for providing timely and unbiased fire-monitoring programs in Alaska as well as other high northern latitudes. Daily data acquisition by moderate- and coarse-resolution instruments provides the only opportunity for developing automated and semi-automated burn mapping approaches that can be produced operationally. However, there are particular challenges to mapping burned areas due to limitations imposed by data availability during and after the completion of the fire season. Our analysis indicates that remote-sensing observations of areas in Alaska and other high northern latitudes are effectively limited to a 5-month period (May through September), with the optimal conditions during June, July and August. However, even during the optimal data collection period, the combined effects of smoke-related high aerosol concentrations, cloud cover and cloud shadow allow for clear observations of only 60–70% of the land area. Smoke is particularly challenging because fires burn for an extended period of time in Alaska and at high northern latitudes. During late-season fires, smoke can often persist until there is snow cover, thus effectively masking the burn until the following year.

A successful approach to dealing with these limitations is presented in the modification of the existing regional algorithm to include pre- and post-fire season spring composites in the overall algorithm processing chain. These composites provide additional information on the spatial extent of the effect of fire on the land surface for late-season fires while still allowing for automated processing of the satellite observations. The presented adjustment to the regional algorithm improved burned area estimates from a Kappa of 0.69 to 0.75 in the 2004 fire season compared with the original algorithm and was able to produce reliable and accurate estimates of burned areas in Alaska between 2004 and 2007.

Acknowledgements

This project was supported by the National Aeronautics and Space Administration through grants NNG05GD25G and NNX08A179G. The authors thank Kelley O'Neal and Carolyn Hight-Harf of the University of Maryland for discussions.

References

- Chen P-Y, Srinivasan R, Fedosejevs G, Kiniry JR (2003) Evaluating different NDVI compositing techniques using NOAA-14 AVHRR data. *International Journal of Remote Sensing* **24**(17), 3403–3412. doi:10.1080/0143116021000021279
- Chuvieco E, Englefield P, Trishchenko AP, Luo Y (2008) Generation of long time series of burn area maps of the boreal forest from NOAA-AVHRR composite data. *Remote Sensing of Environment* **112**(5), 2381–2396. doi:10.1016/j.rse.2007.11.007
- Deng MX, Di LP (2001) Solar zenith angle correction of global NDVI time-series from AVHRR. In 'Proceedings: IEEE International Symposium on Geoscience and Remote Sensing: Scanning the Present and Resolving the Future', 9–13 July 2001, Sydney. Vol. 4, pp. 1838–1840. (Institute of Electrical and Electronics Engineers: New York)
- Eidenshink J, Schwind B, Brewer K, Zhu ZL, Quayle B, Howard S (2007) A project for monitoring trends in burn severity. *Fire Ecology* **3**, 3–21. doi:10.4996/FIREECOLOGY.0301003
- Eva H, Lambin EF (1998) Remote sensing of biomass burning in tropical regions: sampling issues and multisensor approach. *Remote Sensing of Environment* **64**, 292–315. doi:10.1016/S0034-4257(98)00006-6
- Fraser RH, Li Z, Cihlar J (2000) Hotspot and NDVI differencing synergy (HANDS): a new technique for burned area mapping over boreal forest. *Remote Sensing of Environment* **74**(3), 362–376. doi:10.1016/S0034-4257(00)00078-X
- Fraser RH, Hall RJ, Landry R, Lynham T, Raymond D, Lee B, Li Z (2004) Validation and calibration of Canada-wide coarse-resolution satellite burned-area maps. *Photogrammetric Engineering and Remote Sensing* **70**(4), 451–460.
- Giglio L, Descloitres J, Justice CO, Kaufman YJ (2003) An enhanced contextual fire detection algorithm for MODIS. *Remote Sensing of Environment* **87**(2–3), 273–282. doi:10.1016/S0034-4257(03)00184-6
- Giglio L, Loboda T, Roy DP, Quayle B, Justice CO (2009) An active-fire based burned area mapping algorithm for the MODIS sensor. *Remote Sensing of Environment* **113**(2), 408–420. doi:10.1016/j.rse.2008.10.006
- Gillett NP, Weaver AJ, Zwiers FW, Flannigan MD (2004) Detecting the effect of climate change on Canadian forest fires. *Geophysical Research Letters* **31**(18), L18211. doi:10.1029/2004GL020876
- Holben BN (1986) Characteristics of maximum-value composite images from temporal AVHRR data. *International Journal of Remote Sensing* **7**(11), 1417–1434. doi:10.1080/01431168608948945
- Ivanova GA, Ivanov VA, Kukavskaya EA, Soja AJ (2010) The frequency of forest fires in Scots pine stands of Tuva, Russia. *Environmental Research Letters* **5**, 015002. doi:10.1088/1748-9326/5/1/015002
- Kasischke ES, French NHF (1995) Locating and estimating the areal extent of wildfires in Alaskan boreal forest using multiple-season AVHRR NDVI composite data. *Remote Sensing of Environment* **51**, 263–275. doi:10.1016/0034-4257(93)00074-J
- Kasischke ES, Turetsky MR (2006) Recent changes in the fire regime across the North American boreal region – spatial and temporal patterns of burning across Canada and Alaska. *Geophysical Research Letters* **33**, 1–5.
- Kasischke ES, Williams D, Barry D (2002) Analysis of the patterns of large fires in the boreal forest region of Alaska. *International Journal of Wildland Fire* **11**, 131–144. doi:10.1071/WF02023
- Kaufman YJ, Justice CO, Flynn LP, Kendall JD, Prins EM, Giglio L, Ward DE, Menzel WP, Setzer AW (1998) Potential global fire monitoring from EOS-MODIS. *Journal of Geophysical Research – Atmospheres* **103**(D24), 32 215–32 238. doi:10.1029/98JD01644
- Loboda TV, O'Neal KJ, Csiszar IA (2007) Regionally adaptable dNBR-based algorithm for burned area mapping from MODIS data. *Remote Sensing of Environment* **109**, 429–442. doi:10.1016/j.rse.2007.01.017
- López García MJ, Caselles V (1991) Mapping burns and natural reforestation using Thematic Mapper data. *Geocarto International* **6**, 31–37. doi:10.1080/10106049109354290
- Pu R, Li Zh, Gong P, Csiszar I, Fraser R, Hao W-M, Kondragunta S, Weng F (2007) Development and analysis of a 12-year daily 1-km forest fire dataset across North America from NOAA/AVHRR data. *Remote Sensing of Environment* **108**(2), 198–208. doi:10.1016/j.rse.2006.02.027
- Roy DP, Jin Y, Lewis PE, Justice CO (2005) Prototyping a global algorithm for systematic fire-affected area mapping using MODIS time series data. *Remote Sensing of Environment* **97**(2), 137–162. doi:10.1016/j.rse.2005.04.007
- Roy DP, Boschetti L, Justice CO, Ju J (2008) The Collection 5 MODIS burned area product – global evaluation by comparison with the MODIS active fire product. *Remote Sensing of Environment* **112**, 3690–3707. doi:10.1016/j.rse.2008.05.013
- Schott JR (1997) 'Remote Sensing: the Image Chain Approach.' (Oxford University Press: New York)
- Singh SM (1988) Simulation of solar zenith angle effect on global vegetation index (GVI) data. *International Journal of Remote Sensing* **9**(2), 237–248. doi:10.1080/01431168808954848
- Soja AJ, Tchepakova NM, French NH, Flannigan MD, Shugart HH, Stocks BJ, Sukhinin AI, Parfenova EI, Chapin FS, Stackhouse PW (2007) Climate-induced boreal forest change: predictions versus current observations. *Global and Planetary Change* **56**, 274–296. doi:10.1016/j.gloplacha.2006.07.028
- Verbyla DL, Kasischke ES, Hoy EE (2008) Seasonal and topographic effects on estimating fire severity from Landsat TM/ETM+ data. *International Journal of Wildland Fire* **17**, 527–534. doi:10.1071/WF08038
- Vermote EF, Saleous NZ, Justice CO (2002) Atmospheric correction of MODIS data in the visible to middle infrared: first results. *Remote Sensing of Environment* **83**(1–2), 97–111. doi:10.1016/S0034-4257(02)00089-5
- Wolfe RE, Roy DP, Vermote EF (1998) The MODIS land data storage, gridding and compositing methodology: level 2 grid. *IEEE Transactions on Geoscience and Remote Sensing* **36**, 1324–1338. doi:10.1109/36.701082

Manuscript received 2 February 2010, accepted 18 October 2010